Analytical description of z-scan on-axis intensity based on the Huygens–Fresnel principle

Ricardo Elgul Samad and Nilson Dias Vieira, Jr.

Instituto de Pesquisas Energéticas e Nucleares, Caixa Postal 11049, São Paulo 05422-970, Brazil

Received January 27, 1998; revised manuscript received July 27, 1998

An analytical expression capable of calculating the on-axis far-field electric field of a Gaussian beam carrying a phase with a Gaussian profile is obtained. This result is based on the Huygens–Fresnel principle and is not limited to small Gaussian phases. The analytical results are particularized to the z-scan case, agreeing with the Gaussian-decomposition results for small phases. For Gaussian phases with amplitude up to π, a small deviation of the constant peak-to-valley distance is found, but a significant displacement of the axis crossing point is predicted. The theoretical expression of the two-color z-scan is also obtained, and it agrees exactly with the expression obtained by the Gaussian-decomposition method, to first-order approximation. Also we apply our result to the case of a thick sample, verifying the range of coincidence between two different formalisms. © 1998 Optical Society of America [S0740-3224(98)00311-7]

OCIS codes: 190.0190, 190.5940, 190.4420, 140.3460, 260.1960, 350.5030

1. INTRODUCTION

It is well known that self-focusing (or self-defocusing)[1] occurs when a Gaussian laser beam[2] impinges on a sample, owing to its nonlinear refractive index.[3] In this case a Gaussian phase profile is added to the laser wave front. The z-scan technique, introduced by Sheik-Bahae *et al.*,[4] is based on the measurement of this nonlinear phase and provides a simple (single beam) and sensitive method to measure both the real and the imaginary parts of the complex nonlinear refractive index of a sample. In the basic technique a thin sample is moved along the axis of a TEM_{00} laser beam, throughout its waist, which originates a Gaussian modulation of the refractive index of the sample. This refractive-index change acts on the laser beam, producing an intensity change in an iris located in the far field, providing a correlation between the intensity and the nonlinear refractive index of the sample.

Many modifications of the method have been proposed since its introduction. Such modifications include those aimed at improving the single-beam method,[5–9] those that use a pump and a probe beam[10,11] to measure diagonal terms[12] of the third-order nonlinearity, and the use of a method to investigate the excited-state properties of some doped crystals.[13,14] The analysis of the detected intensity also was investigated by means of various theoretical models based on the Huygens–Fresnel formalism,[15] the Gaussian-decomposition,[16] (GD) and the fast-Fourier-transform[17] (FFT) and complex ray-tracing[18] methods. Also, analytical solutions were found, in the first-order approximation, for the on-axis normalized transmittance for the weak nonlinear regime, for thin and thick media.[19,20]

The basic equations governing the intensity variation and the accumulated nonlinear phase inside the sample are given by

$$\frac{\mathrm{d}I}{\mathrm{d}z'} = -\alpha I, \tag{1}$$

$$\frac{\mathrm{d}(\Delta\phi)}{\mathrm{d}z'} = \delta n(I)k, \tag{2}$$

where α is the sample linear absorption coefficient, z' is the coordinate inside the sample, k is the wave number of the laser, and $\delta n(I)$ is the refractive-index variation owing to the laser intensity, I. In the simplest case this variation is proportional to the intensity, and we denote $\delta n(I) = n_2 I$, where n_2 is the nonlinear refractive index of the sample. The solution of these equations when the pumping beam has a TEM_{00} electric-field distribution[2] gives the electric field in the exit plane of the sample, E_S:

$$E_s(z, r) = E_0 \frac{w_0}{w(z)} \exp(-\alpha L/2)\exp\left[-\frac{r^2}{w(z)^2} - i\frac{kr^2}{2R(z)} - ikz\right]\exp\left\{-i\Delta\phi_0 \exp\left[-\frac{2r^2}{w(z)^2}\right]\right\}. \tag{3}$$

In Eq. (3), E_0 is the beam-waist electric-field amplitude, w_0 is the beam waist (at $z = 0$), L is the sample length, r is the radial distance from the axis of the beam, and z is the position of the sample relative to the position of the beam waist. The parameters $w(z)$ and $R(z)$ are the waist and the curvature radius of the wave front for a Gaussian laser beam.[2] The first exponential represents the beam attenuation owing to the sample absorption; the second expresses the electric-field amplitude distribution and the intrinsic phase of the laser wave front. The last exponential is the term with the nonlinear phase, $\Delta\phi_0$, whose distribution follows a Gaussian profile. The nonlinear phase amplitude is modulated by the beam size and is given by

$$\Delta\phi_0 = \frac{kn_2 L_{\mathrm{eff}} I_0}{(1 + z^2/z_0^2)} = \frac{\Delta\Phi_0}{(1 + z^2/z_0^2)}, \tag{4}$$

where $L_{\mathrm{eff}} = [1 - \exp(-\alpha L)]/\alpha$ is the sample effective length, I_0 is the laser intensity at the beam waist, z_0 is

0740-3224/98/112742-06$15.00

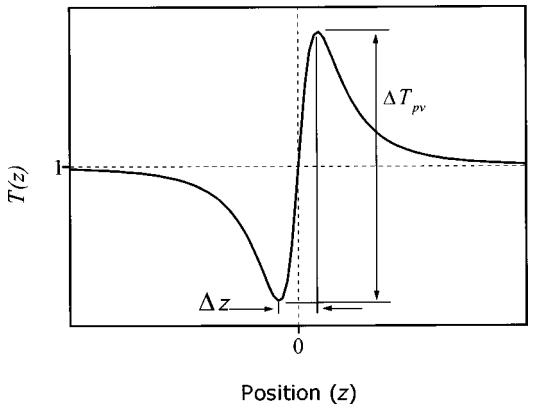

Fig. 1. Parameters of a z-scan curve for a sample with a positive nonlinearity.

the confocal parameter of the beam, and $\Delta\Phi_0$ is the nonlinear phase at the beam-waist position.

The traditional z-scan analysis is based on the GD method proposed by Weaire *et al.*[16] This method allows for the calculation of the electric field in the plane of the iris as a sum over infinite Gaussian beams. If the iris aperture and the nonlinear phase introduced are sufficiently small ($\Delta\Phi_0 < \pi$), we can disregard second-order and higher terms in the sum and calculate the electric field in $r = 0$. Sheik-Bahae *et al.* calculated the normalized transmittance through the aperture, $T(z)$, defined by the ratio between the intensities of the nonlinear phase carrier beam, and a reference beam, which is not affected by the nonlinear phase. With these approximations the normalized transmittance is given by

$$T(z) = 1 + \frac{4\Delta\Phi_0 x}{(x^2 + 1)(x^2 + 9)} \tag{5}$$

with $x = z/z_0$. The curve described by Eq. (5) is shown in Fig. 1. Under these approximations the transmittance variation between peak and valley (ΔT_{pv}) and the distance between peak and valley (Δz) are given by

$$\Delta T_{\mathrm{pv}} = 0.406|\Delta\Phi_0|, \tag{6}$$

$$\Delta z = 1.72 z_0. \tag{7}$$

This theory is valid for peak–valley transmittance variations of ~20%, corresponding to nonlinear phases smaller than π.[4] For greater phases, more terms are needed in the sum, thus limiting the simplicity of the method.

2. THEORY

We present here a model developed to deal with phases with a Gaussian profile of arbitrary magnitude, carried by a Gaussian laser beam, allowing the prediction of the electric field in the optical axis. The theory is exact for Gaussian phase profiles, and it comprehends all the summation series of Eq. (9) from Ref. 4, for the on-axis approximation.

To describe the model, we refer to Fig. 2. This model is based on the propagation of a wave front by means of the Fresnel diffraction integral and use of the Huygens–Fresnel principle.[21] Therefore each point in a wave front may be considered as the center of a perturbation that originates a spherical wave (Huygens principle), and all these secondary spherical waves will interfere to define the wave front in another position (Fresnel principle).

In the model the center of the thin sample (S) is the origin of the cylindrical coordinates (ρ, θ). We considered a nonlinear sample at the position z, with a Gaussian laser beam impinging on it. This provides a nonlinear Gaussian phase profile that is added to the original beam phase, and we must take it into account to calculate the on-axis electric field at the point C, after a propagation distance d. The distance between the beam waist and the observation point, C, is D.

The electric field at the sample exit plane is given by Eq. (3). To determine the electric field at point C, we must calculate the contribution of each spherical-wave source for this expression. This is done multiplying Eq. (3) by the Huygens propagation term, W, over a distance r:

$$W = \frac{ik}{2\pi}\frac{\exp(-ikr)}{r}, \tag{8}$$

where $r = |\mathbf{r}|$ is the distance from the center of the spherical wave to the point C. The electric field at point C is then given by the sum, or integral, of all the spherical waves originating at the sample exit plane:

$$E_C(z) = \frac{ik}{2\pi}\int_0^{2\pi} \mathrm{d}\theta \int_0^{\infty} \mathrm{d}\rho\rho E_S(z, \rho)\frac{\exp(-ikr)}{r}. \tag{9}$$

To calculate the integral, as $d \gg \rho$, we can approximate the distance r by

$$r = \sqrt{d^2 + \rho^2} \cong d + \frac{1}{2}\frac{\rho^2}{d}. \tag{10}$$

This is the standard paraxial approximation, in which we keep Eq. (10) in the phase term, which is compared with λ, and we use $r \approx d$ for the amplitude term. Changing the variables according to

$$\alpha = \left\{\frac{1}{w(z)^2} + i\frac{k}{2}\left[\frac{1}{R(z)} + \frac{1}{d}\right]\right\}, \tag{11}$$

$$\beta = \frac{2}{w(z)^2},$$

$$\Lambda = ikE_0\frac{w_0}{w(z)}\exp(-\alpha L/2 - ikD)\frac{1}{d},$$

we can write the integral to be solved as

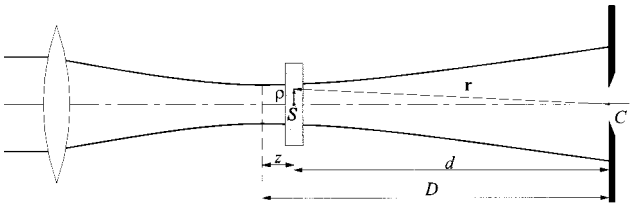

Fig. 2. Scheme of the coordinates utilized in the calculation of the Fresnel integral.

$$E_C = \Lambda \int_0^\infty \mathrm{d}\rho\rho \, \exp(-\alpha\rho^2)\exp[-i\Delta\phi_0 \, \exp(-\beta\rho^2)]. \tag{12}$$

The difficulty in integrating Eq. (12) resides in its last term, where there is an exponential of an exponential. In order to solve it, we make the substitutions $\xi = \beta\rho^2$ and $\exp(-\xi) = \zeta$, obtaining an expression to be integrated in the variable ζ. Substituting $\mu(z) = (\alpha/\beta) - 1$ and $\nu = i\Delta\phi_0\zeta$, Eq. (12) is reduced to

$$E_C = \frac{\Lambda}{2\beta(i\Delta\phi_0)^{\mu+1}} \int_0^{i\Delta\phi_0} \mathrm{d}\nu\nu^\mu \exp(-\nu). \tag{13}$$

Equation (13) is the integral representation of the incomplete gamma function[22]:

$$\Gamma(\mu + 1, a, b) = \int_a^b \mathrm{d}\nu\nu^\mu \exp(-\nu). \tag{14}$$

Now we can define the variable $\gamma(z)$ as

$$\gamma(z) = \mu(z) + 1 = \frac{1}{2}\left[\frac{i}{z_0}\left(z + \frac{z^2 + z_0^2}{d}\right) + 1\right]. \tag{15}$$

With this definition the electric field at point C is given, in the paraxial approximation, by

$$E_C(z, i\Delta\phi_0) = \left[i \frac{\pi}{2\lambda} E_0 \exp(-\alpha L/2 - ikD) \frac{w_0^2}{d}\right] \times [1 + (z/z_0)^2]^{1/2} \frac{\Gamma(\gamma, 0, i\Delta\phi_0)}{(i\Delta\phi_0)^\gamma}. \tag{16}$$

For experimental purposes we must calculate the intensity of the laser beam, given by $I_C = E_C^* E_C$, where E_C^* is the conjugate of the electric field. To obtain the normalized intensity, I_C^N, we must calculate the ratio $I_C(\Delta\phi_0)/I_C(\Delta\phi_0 \to 0)$. The limit of $\Gamma(\gamma, 0, i\Delta\phi_0)/(i\Delta\phi_0)^\gamma$ at point C, when the nonlinear phase approaches zero, is $1/(i\gamma)$, and consequently, the normalized intensity at point C is

$$I_C^N(z, i\Delta\phi_0) = \left|\gamma(z) \frac{\Gamma(\gamma, 0, i\Delta\phi_0)}{(i\Delta\phi_0)^\gamma}\right|^2. \tag{17}$$

3. APPLICATION OF THE THEORY OF THE INCOMPLETE GAMMA FUNCTION TO THE Z-SCAN TECHNIQUE

To obtain the normalized transmittance for the z scan, we must calculate Eqs. (17) and (15) with the adequate γ and $\Delta\Phi_0$ for this method. In this case we only have to substitute the nonlinear phase and the distance to the iris (point C), which varies in the z scan. The substitutions are $d = D - z$ and $\Delta\phi_0 = \Delta\Phi_0/[1 + (z/z_0)^2]$, and we obtain

$$T(z, \Delta\Phi_0) = \left| \gamma(z) \frac{\Gamma\left[\gamma(z), 0, i \dfrac{\Delta\Phi_0}{1 + (z/z_0)^2}\right]}{\left[i \dfrac{\Delta\Phi_0}{1 + (z/z_0)^2}\right]^{\gamma(z)}} \right|^2, \tag{18a}$$

$$\gamma(z) = \frac{1}{2}\left[\frac{i}{z_0}\left(z + \frac{z^2 + z_0^2}{D - z}\right) + 1\right]. \tag{18b}$$

With the expansion[23] of the incomplete gamma function,

$$\Gamma(\mu, 0, x) = \int_0^x \mathrm{d}\nu\nu^{\mu-1}e^{-\nu} = x^\mu \sum_{n=0}^{\infty} (-1)^n \frac{x^n}{n!(\mu + n)} \tag{19}$$

in Eq. (18a), to first order ($n = 1$) the normalized transmittance is given by

$$T^{(1)}(z) = \left|1 - \frac{i\Delta\phi_0(z)}{1 + 1/\gamma(z)}\right|. \tag{20}$$

After some simplifications, and disregarding terms of second order, we obtain

$$T^{(1)}(z) = 1 + 4\Delta\phi_0 \frac{x[1 + z/d(1 + 1/x^2)]}{9 + x^2[1 + z/d(1 + 1/x^2)]} \tag{21}$$

with $x = z/z_0$. In the condition $d \gg z$, Eq. (21) converges to Eq. (5), calculated by the GD theory for small phases.

Another direct application of Eqs. (18a) and (18b) is to calculate the normalized transmittance for the case of the two-color z scan. In this case, two laser beams are utilized: the probe beam with parameters w, z_0, and k, and the pump beam, with parameters w_p, z_{p0}, and k_p, aligned collinearly, with their waist positions coinciding. The sample is moved along the optical axis, and in this case Eqs. (18a) and (18b) are modified to

$$T(z, \Delta\Phi_0) = \left| \gamma(z) \frac{\Gamma\left[\gamma(z), 0, i \dfrac{\Delta\Phi_0}{1 + (z/z_{p0})^2}\right]}{\left[i \dfrac{\Delta\Phi_0}{1 + (z/z_{p0})^2}\right]^{\gamma(z)}} \right|^2,$$

$$\gamma(z) = \frac{1}{2}\frac{w_p^2}{w^2}\left[\frac{i}{z_0}\left(z + \frac{z^2 + z_0^2}{D - z}\right) + 1\right]. \tag{22}$$

Calculating the normalized transmittance for small phases, as done previously with the expansion of the gamma function, the on-axis normalized transmittance converges to Eq. (6) given by Ma *et al.*[24]:

$$T^{(1)}(z) = 1 + \frac{4a^2bx\Delta\Phi_0}{(a + 2b + ax^2)^2 + 4a^2b^2x^2}, \tag{23}$$

where $x = z/z_{p0}$, $a = z_{p0}/z_0$, and $b = k_p/k$.

4. COMPARISON WITH CURRENT THEORIES

The theory of the incomplete gamma function (TIGaF) is general and exact. It enables the calculation of the intensity in the optical axis on the far field, for any magnitude of the phase, as long as it keeps a Gaussian profile. In order to perform this calculation we need only to identify the on-axis Gaussian phase, $\Delta\phi_0$, and the parameters α and β (the amplitude and the phase distribution of

the Gaussian beam plus the propagation term $ik/2d$, and the width of the Gaussian phase profile) of Eqs. (11), in the beam of interest, and substitute them in the expression the gamma function. An analytical solution for the normalized transmittance, for the near and far fields, was also obtained for any radial symmetry profile of the nonlinear phase by Hermann *et al.*[20] This solution is valid for weak nonlinearities, on first-order approximation. In the range of validity of this theory, as long as the Gaussian profile of the phase is maintained, it coincides with the present theory, which corresponds to consideration of thin samples. The main advantage of this theory[20] is that it comprises any radial profile, in the near and far fields, but is limited to weak nonlinearities, and the present theory is valid for any magnitude of the phase, but is restricted to Gaussian phases. The range of coincidence of the theories, in the weak nonlinear regime, is for samples with thickness up to 40% of the confocal parameter of the laser beam, implying that, for samples within this thickness, the nonlinear phase keeps the Gaussian profile. In Appendix A the interplay of the present theory and the analytical one developed by Hermann *et al.*[20] is described.

5. ANALYTICAL SIMULATIONS

Figure 3 shows analytical curves resulting from GD theory [Eq. (5), shown by the dashed curve] and TIGaF [Eq. (18a), shown by the solid curve], for a small nonlinear phase ($\pi/100$) caused by a positive nonlinearity. The results are parameterized in terms of the confocal parameter (z_0) of the laser beam without loss of generality. The two curves overlap almost exactly in the whole interval, showing a good agreement between the two theories, and the TIGaF prevision is almost symmetric, crossing the axis $T(z) = 1$ at $z \cong 0$. Figure 4 shows the analytical results of GD (dashed curves) and TIGaF (solid curves) for the nonlinear phases $\Delta\Phi_0$ equal to $\pi/4$, $\pi/2$ and π. As the nonlinear phase increases, we note that the TIGaF-predicted curve become asymmetric, and the point where it crosses the axis $T(z) = 1$ moves away from the zero toward the positive portion of the axis. The position of the point $T(z) = 1$ as a function of the nonlinear phase is shown in Fig. 5. The displacement of the point

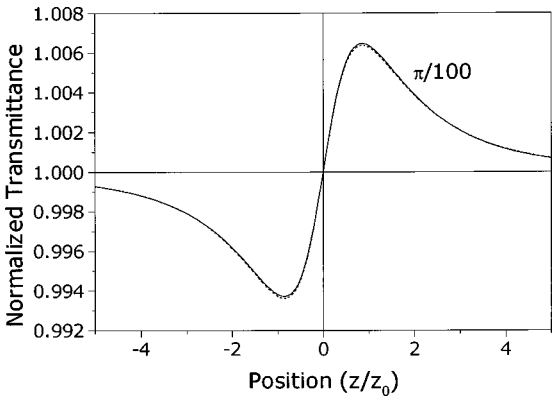

Fig. 3. Comparison between the previsions of GD theory (dashed curve) and TIGaF (solid curve) for small nonlinear phases. Shown are the curves for a nonlinear phase equal to $\pi/100$.

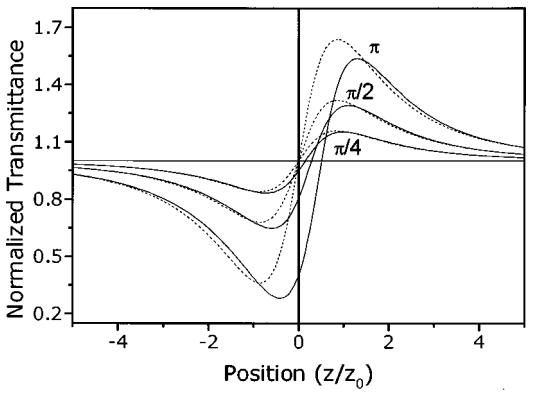

Fig. 4. Comparison between the previsions of GD theory (dashed curves) and TIGaF (continuous curves) for great nonlinear phases. The graph depicts the results for $\Delta\Phi_0$ equals $\pi/4$, $\pi/2$ and π.

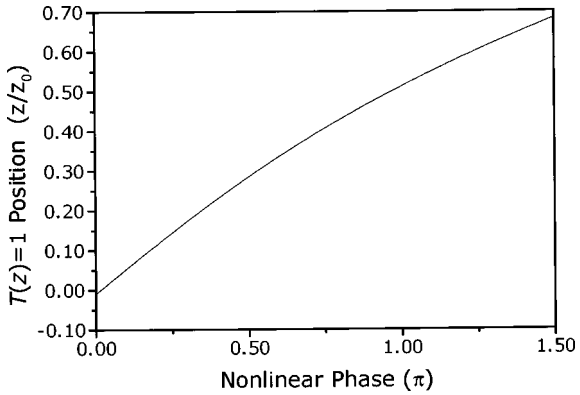

Fig. 5. Position of the point where the z-scan curve crosses the axis $T(z) = 1$ as a function of the nonlinear phase.

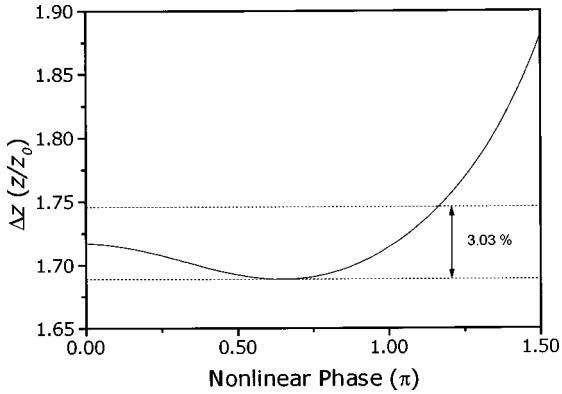

Fig. 6. Peak–valley distance as a function of the nonlinear phase; for phases up to 1.15π the error in $\Delta z = 1.72z_0$ is smaller than 1.5%.

$T(z) = 1$ toward the positive portion of the axis can be explained by the focusing lens effect. For a thin sample at the waist position ($z = 0$), for a small pumping intensity, a weak nonlinear positive lens is induced, increasing the normalized transmittance. This effect moves the point of $T(z) = 1$ to negative positions, as seen in the graph of Fig. 5. As the pumping intensity increases, a stronger lens effect is induced in the sample, originating a strong focusing of the beam, with a smaller waist than the original, very close to the sample. As a consequence,

there is a decrease of the normalized transmittance, moving the crossing point to positive portions of the axis.

Figure 6 presents the distance between peak and valley as a function of the nonlinear phase. For small phases this distance is constant and has the value $1.72z_0$, as shown by Sheik-Bahae.[4] As the pumping intensity increases, the distance between peak and valley decreases, reaching a minimum of approximately $1.69z_0$ (1.7% of variation) for a nonlinear phase of $\sim 0.65\pi$. Above this value, the peak–valley distance increases monotonically with the nonlinear phase.

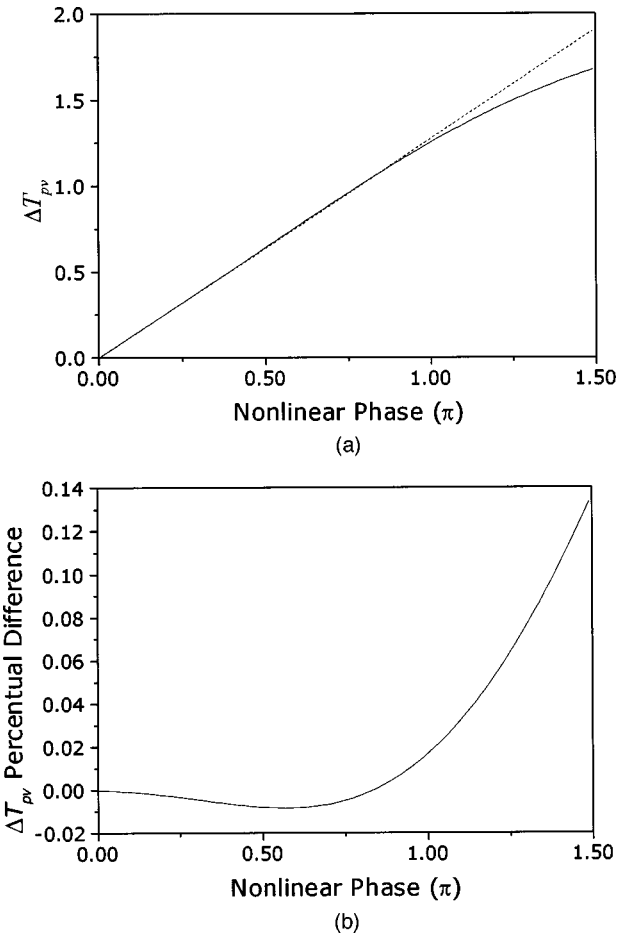

Fig. 7. (a) Comparison between the TIGaF ($\Delta T_{\mathrm{pv-\Gamma}}$, solid curve) and GD ($\Delta T_{\mathrm{pv-GD}}$ dashed curve) previsions for the transmittance variation between peak and valley. (b) Percentage difference $(\Delta T_{\mathrm{pv-GD}} - \Delta T_{\mathrm{pv-\Gamma}})/\Delta T_{\mathrm{pv-\Gamma}}$.

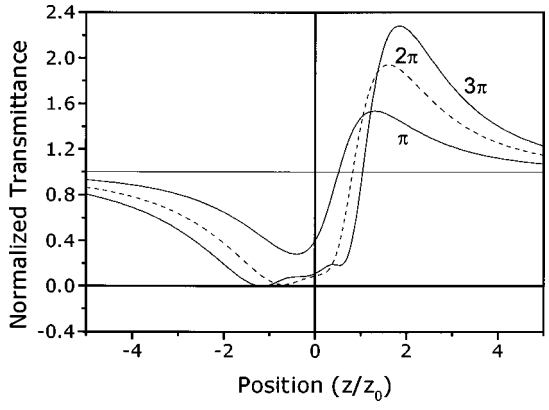

Fig. 8. TIGaF prevision for z-scan curves with large ($\geq\pi$) nonlinear phases. The curves represent the results for nonlinear phases equal to π, 2π, and 3π.

The important parameter to determine the nonlinearity is the transmittance variation between peak and valley. In Fig. 7 this variation is shown as a function of the nonlinear phase. In (a) the dashed curve represents the result from GD theory, Eq. (6), and the solid curve shows the TIGaF prevision. In (b) is shown the percentage difference between TIGaF and GD previsions. In this graphic we can see that the difference between the previsions is under 2% for a nonlinear phase equal to π. The results obtained are analogous when the sample has a negative nonlinearity.

For nonlinear phases greater than π (in modulus) the results cannot be described by the GD theory in the form of Eq. (5), and the peak–valley transmittance difference departs from Eq. (6). Figure 8 shows the previsions of TIGaF for nonlinear phases equal to π, 2π, and 3π. For a nonlinear phase equal to π there is already a noticeable asymmetry around the origin in the curve, which becomes more pronounced as the pumping intensity increases. For nonlinear phases equal to or greater than 2π there are oscillations in the curve, and the normalized transmittance almost reaches a value equal to zero, showing an almost total destructive interference in the optical axis. The point of minimum of the z-scan curve is displaced to negative positions as the nonlinear phase increases. This happens because the destructive interference is reached with the sample more distant from the beam waist, as can be seen in the curve for $\Delta\Phi_0 = 3\pi$. The saturation of the peak–valley distance predicted by the TIGaF, observed in Fig. 7(a), occurs because of this destructive interference occurring for large nonlinear phases.

6. CONCLUSIONS

Using the Huygens–Fresnel principle, we found an analytical solution for the propagation of a Gaussian laser beam electric field. The particular solution found is valid whenever a Gaussian phase profile is added to the laser intrinsic phase and is given in terms of the well-known incomplete gamma function. This solution is capable of calculating the electric field on the optical axis of the laser beam, for any magnitude of the Gaussian phase profile.

The solution was particularized for the z-scan case, where the phase is modulated by the laser beam and is then propagated to an iris in the far field. We could show that for small nonlinear phases our predictions agree with the GD method. Our developments are valid for nonlinear phases greater than π, showing several modifications on the z-scan curve. We also showed that the solution found could be particularized for the two-color z scan, where a laser originates the nonlinear phase and another laser beam carries it. In this case we calculated the solution when the waist positions of the two beams are coincident.

APPENDIX A: COMPARISON OF THE PRESENT THEORY TO THE FIRST-ORDER APPROXIMATION FOR THICK MEDIA

By defining, according to Hermann *et al.*,[20] the following parameters for the z-scan case,

$$\gamma = (1 + \zeta_0^2),$$
$$\mu = (1 - \zeta_0\zeta_m/\gamma)^2 + (\zeta_m/\gamma)^2,$$
$$\zeta_0 = z/z_r,$$
$$\zeta_m = L/z_r,$$
$$u = [2\exp(2iy) - 1]^{-1},$$
$$y = \arctan(\zeta_0) + \arctan(\zeta_m - \zeta_0), \tag{A1}$$

where r_0 is the beam waist and z_r is the Rayleigh length of the laser beam, L is the sample thickness, and b is the nonlinearity, we can express the parameters α, $\Delta\phi_0$, and β of our theory as

$$\alpha = \frac{1}{\gamma\mu r_0^2}[1 + i(\zeta_0 - \zeta_m)] + i\frac{k}{2d},$$
$$\Delta\phi_0 = \frac{b}{8}\,\mathrm{Re}[i\,\ln(u^{-1})],$$
$$\beta = \frac{b}{4\Delta\phi_0\gamma\mu r_0^2}\,\mathrm{Re}[i(1 - u)]. \tag{A2}$$

These parameters should be used in Eqs. (15) and (17) above to obtain the z-scan curve by varying the sample position, z (or ζ_0).

ACKNOWLEDGMENTS

We thank Fundação de Amparo à Pesquisa do Estado de São Paulo (FAPESP), a state-founding agency, for supporting this work (FAPESP grant 93/4999-7). R. E. Samad also thanks FAPESP for a scholarship (FAPESP 93/1367-0).

REFERENCES

1. Y. R. Shen, *The Principles of Nonlinear Optics* (Wiley, New York, 1984), Chap. 17.
2. H. Kogelnik and T. Li, Appl. Opt. **5**, 1550 (1966).
3. R. Adair, L. L. Chase, and S. A. Payne, Phys. Rev. B **39**, 3337 (1989).
4. M. Sheik-Bahae, A. A. Said, T. Wei, D. J. Hagan, and E. W. Van Stryland, IEEE J. Quantum Electron. **26**, 760 (1990).
5. T. Xia, D. J. Hagan, M. Sheik-Bahae, and E. W. Van Stryland, Opt. Lett. **19**, 317 (1994).
6. W. Zhao and P. Palffy-Muhoray, Appl. Phys. Lett. **63**, 1613 (1993).
7. J.-G. Tian, W.-P. Zang, and G. Zhang, Opt. Commun. **107**, 415 (1994).
8. R. E. Bridges, G. L. Fischer, and R. W. Boyd, Opt. Lett. **20**, 1821 (1995).
9. B. K. Rhee and J. S. Byun, J. Opt. Soc. Am. B **13**, 2720 (1996).
10. H. Ma, A. S. L. Gomes, and C. B. de Araujo, Appl. Phys. Lett. **59**, 2666 (1991).
11. M. Sheik-Bahae, J. Wang, R. DeSalvo, D. J. Hagan, and E. W. Van Stryland, Opt. Lett. **17**, 258 (1992).
12. P. N. Butcher and D. Cotter, *The Elements of Nonlinear Optics* (Cambridge U. Press, Cambridge, UK, 1993), Chap. 4.
13. T.-H. Wei, T.-H. Huang, and H.-D. Lin, Appl. Phys. Lett. **67**, 2266 (1995).
14. L. C. Oliveira, T. Catunda, and S. C. Zilio, Jpn. J. Appl. Phys. **35**, 2649 (1996).
15. M. Sheik-Bahae, A. A. Said, D. J. Hagan, M. J. Soileau, and E. W. Van Stryland, Opt. Eng. **30**, 1228 (1991).
16. D. Weaire, B. S. Wherrett, D. A. B. Miller, and S. D. Smith, Opt. Lett. **4**, 331 (1979).
17. S. Hughes, J. M. Burzler, G. Spruce, and B. S. Wherrett, J. Opt. Soc. Am. B **12**, 1888 (1995).
18. W. Nasalsky, Opt. Commun. **119**, 218 (1995).
19. J. A. Hermann, Int. J. Nonlinear Opt. Phys. **1**, 541 (1992).
20. J. A. Hermann and R. G. McDuff, J. Opt. Soc. Am. B **10**, 2056 (1993).
21. M. Born and E. Wolf, *Principles of Optics*, 5th ed. (Pergamon, New York, 1975), Chap. 8.
22. M. Abramowitz and I. A. Stegun, *Handbook of Mathematical Functions With Formulas, Graphs and Mathematical Tables*, 10th ed. (Ntl. Bur. Stand., Gaithersburg, Md., 1972), Chap. 6.
23. G. B. Arfken and H. J. Weber, *Mathematical Methods for Physicists*, 4th ed. (Academic, San Diego, 1995), Chap. 10.
24. H. Ma and C. B. de Araujo, Appl. Phys. Lett. **66**, 1581 (1995).